HHS Public Access

Author manuscript

Toxicol Appl Pharmacol. Author manuscript; available in PMC 2016 October 05.

Published in final edited form as:

Toxicol Appl Pharmacol. 2010 June 1; 245(2): 226–235. doi:10.1016/j.taap.2010.03.004.

Cr(VI) induces mitochondrial-mediated and caspase-dependent apoptosis through reactive oxygen species-mediated p53 activation in JB6 Cl41 cells

Young-Ok Son[a], **J. Andrew Hitron**[a], **Xin Wang**[a], **Qingshan Chang**[a], **Jingju Pan**[a], **Zhuo Zhang**[a], **Jiankang Liu**[a], **Shuxia Wang**[b], **Jeong-Chae Lee**[c,d], and **Xianglin Shi**[a,*]

[a]Graduate Center for Toxicology, University of Kentucky, Lexington, KY 40536-0305, USA

[b]Graduate Center for Nutritional science, College of Medicine, University of Kentucky, Lexington, KY 40536-0305, USA

[c]School of Dentistry and 21 Century Education Center for Advanced Public Dental Health (BK 21 program), Chonbuk National University, Jeonju 561-756, South Korea

[d]Research Center of Bioactive Materials, Chonbuk National University, Jeonju 561-756, South Korea

Abstract

Cr(VI) compounds are known to cause serious toxic and carcinogenic effects. Cr(VI) exposure can lead to a severe damage to the skin, but the mechanisms involved in the Cr(VI)-mediated toxicity in the skin are unclear. The present study examined whether Cr(VI) induces cell death by apoptosis or necrosis using mouse skin epidermal cell line, JB6 Cl41 cells. We also investigated the cellular mechanisms of Cr(VI)-induced cell death. This study showed that Cr(VI) induced apoptotic cell death in a dose-dependent manner, as demonstrated by the appearance of cell shrinkage, the migration of cells into the sub-G1 phase, the increase of Annexin V-positively stained cells, and the formation of nuclear DNA ladders. Cr(VI) treatment resulted in the increases of mitochondrial membrane depolarization and caspases activation. Electron spin resonance (ESR) and fluorescence analysis revealed that Cr(VI) increased intracellular levels of reactive oxygen species (ROS) such as hydrogen peroxide and superoxide anion radical in dose-dependent manner. Blockage of p53 by si-RNA transfection suppressed mitochondrial changes of Bcl-2 family composition, mitochondrial membrane depolarization, caspase activation and PARP cleavage, leading to the inhibition of Cr(VI)-induced apoptosis. Further, catalase treatment prevented p53 phosphorylation stimulated by Cr(VI) with the concomitant inhibition of caspase activation. These results suggest that Cr(VI) induced a mitochondrial-mediated and caspase-dependent apoptosis in skin epidermal cells through activation of p53, which are mainly mediated by reactive oxidants generated by the chemical.

*Corresponding author. Tel: +1-859-257-4054; Fax: +1-859-323-1059; xshi5@email.uky.edu.

Keywords

Cr(VI); p53; Reactive oxygen species (ROS); Apoptosis; Mitochondrial stress

Introduction

Serious toxic and carcinogenic chemicals, chromate (Cr(VI)) compounds, are widely used in industry (Cohen et al., 1993; Costa, 1997). More than 300,000 workers in the United States are potentially exposed to Cr(VI) and Cr(VI)-containing compounds in the workplace. When environmental contamination of these compounds occurs, living organisms are exposed to the chemicals by air, water, and food, or by direct contact to the skin. Cr(VI) enters the body by inhalation, ingestion, or absorption through the skin. For occupational exposure, the airways and skin are the primary routes of uptake (Costa, 1997; Shelnutt et al., 2007). Occupational exposure to Cr(VI) is a well-established cause of skin damage such as skin ulcers and irritant contact dermatitis, and delayed hypersensitivity reactions (Hansen et al., 2006; Shelnutt et al., 2007). Also, Cr(VI) has allergenic potential cause skin eczema and atopic dermatitis (Hansen et al., 2006). Recently, it has been reported that Cr(VI) induce dermal toxicity (Joseph et al., 2008; Shelnutt et al., 2007).

Hexavalent chromium (Cr(VI)) and trivalent chromium (Cr(III)) are two stable chromium oxidation states found in nature. Cr(VI) is able to enter into cells through an anion transport system (Connett and Wetterhahn, 1983). Once inside cells, it is reduced by cellular reductants to its lower oxidation states, pentavalent chromium (Cr(V)) and tetravalent chromium (Cr(IV)) (Shi et al., 1999). These intermediate states of chromium are reactive to produce reactive oxygen species (ROS) (Shi and Dalal, 1989, 1990c) which are known to cause oxidative damages such as DNA strand breaks, base modification and lipid peroxidation (Ding and Shi, 2002; Hodges et al., 2001; Shi et al., 1999; Stohs et al., 2000; Xu et al., 1992; Ye et al., 1995). Thus it is generally believed that Cr(VI) could induce cell death by oxidative stress (Blankenship et al., 1994; D'Agostini et al., 2002; Flores and Perez, 1999; Shimada et al., 1998).

Oxidative stress can cause cell death ether by apoptosis or necrosis. Unlike necrotic cell death, apoptotic cell death is a process controlled tightly by a specific signaling pathway (Shimada et al., 1998; Waalkes et al., 2000) and is characterized by cellular shrinkage, nuclear condensation, and DNA fragmentation (Kroemer and Reed, 2000; Li et al., 1997; Susin et al., 1999). Numerous studies have demonstrated that the mitochondria stress and caspase activation are the most typical events required for apoptosis (Ghelli et al., 2003). There are also accumulating evidence to show the mode of cell death induced by oxidative stress; the death modes are differently affected according to the types of cells examined and the methods to generate ROS, i.e., continuous generation versus bolus addition (Barbouti et al., 2007; Barbouti et al., 2002; Son et al., 2009a; Son et al., 2009b).

Although ROS is thought to be related to Cr(VI)-mediated cell death, the precise mechanisms by which Cr(VI) induces apoptosis in cultured skin cells have not been elucidated. In this study, we examined whether Cr(VI) induces apoptosis using mouse skin epidermal cell line, JB6 Cl41 cells. We also investigated the cellular mechanisms of Cr(VI)-

induced cell death. We have demonstrated that Cr(VI)-stimulated ROS production leads to mitochondrial-mediated and caspase-dependent apoptosis through activation of p53 in the cells.

Materials and methods

Chemicals and laboratory wares

Unless specified otherwise, all chemicals and laboratory wares were purchased from Sigma Chemical Co. (St. Louis, MO) and Falcon Labware (Bectone-Dickinson, Franklin Lakes, NJ). Eagle's minimal essential medium (EMEM), FBS, gentamicin, and L-glutamine were purchased from Gibco Co. (Gibco BRL, NY). 5-(and-6)-chloromethyl-2',7'-dichlorodihydrofluorescein diacetate, acetyl ester (CM-H_2DCFDA), and dihydroethidium were obtained from Molecular Probes (Eugene, OR). Superoxide dismutase (SOD) and *N*-(4-hydroxyphenyl) retinamide (4HPR) were purchased from Calbiochem (San Diego, CA)

Cell culture and treatment

The JB6 P^+ mouse epidermal cell line, Cl 41 cells (ATCC, CRL-2010) were cultured in EMEM containing 5% FBS, 2 mM L-glutamine, and 50 μg of gentamicin/ml. The cells were grown at 37 °C in a 5% CO_2 atmosphere. One million cells per milliliter were resuspended in either 3 ml or 200 μl of the media before spreading onto either 60 mm culture dish or 96-well culture plates, respectively. After the cell had reached 80% confluence, culture medium was replaced with a fresh medium containing 0.5% FBS and various concentrations (0–10 μM) of $Na_2Cr_2O_7$.

Measurements of cell viability and cytotoxicity

3-(4,5-dimethylthiazol-2yl-)-2,5-diphenyl tetrazolium bromide (MTT) was used to evaluate viability of cells. JB6 cells were cultured in EMEM supplemented with 0.5% FBS in the presence of 0 to 10 μM of Cr(VI) ($Na_2Cr_2O_7$), 500 U/ml catalase (CAT), 500 U/ml SOD, 100 μM deferoxamine (DFX) and/or 10 mM sodium formate (SF). After 48 h of incubation, 5 μl of a MTT solution (5 mg/ml in PBS as stock solution) was added into each well of 96-well plates, and incubated for additional 4 h at 37 °C. MTT-reducing activity of cells was measured by treating them with acidic isopropanol prior to reading at 560 nm with Spectra Max Plus^{384} (Molecular Devices, Sunnyvale, CA). In addition, cellular cytotoxicity was measured using a trypan blue exclusion assay. The cytotoxicity was calculated as follows: % cytotoxicity = [(total cells - viable cells)/total cells] × 100%.

FITC-annexin V/propidium iodide (PI) staining

JB6 cells were washed twice with PBS before being suspended in 1× binding buffer (10 mM Hepes, pH 7.4, 140 mM NaOH, 2.5 mM $CaCl_2$). Five μl of FITC-labeled annexin V were mixed with 100 μl of cell suspensions containing 1×10^5 cells, and the cells were incubated at room temperature for 10 min. Afterward, 2 μl of PI solution (10 μg/ml) was added into the cells followed by additional 10 min incubation on ice. The scatter parameters of the cells (20,000 cells per experiment) were analyzed using a FACS Calibur® system. Four cell populations were identified according to the following interpretation: viable population in the lower-left quadrant (low PI and FITC signals); early apoptotic population in the lower-

right quadrant (low PI and high FITC signals); necrotic population in the upper-left quadrant (high PI and low FITC signals); and late apoptotic or necrotic population in the upper-right quadrant (high PI and high FITC signals).

Agarose gel electrophoresis

Cells were incubated with a lysis buffer (1% NP-40 and 1% SDS in 50 mM Tris-HCl, pH 8.0) at 65 °C for 1 h. DNA was extracted with phenol/chloroform/isoamyl alcohol, and the aqueous phase was precipitated overnight with 2 volumes of ethanol at −20 °C. The pellet was air-dried and resuspended in TE buffer (10 mM Tris-Cl and 1 mM EDTA, pH 8.0). The degree of fragmentation was analyzed using 2% agarose gel electrophoresis followed by ethidium bromide staining.

Western blot analyses

Cell lysates were made in a lysis buffer (50 mM Tris-Cl, pH 7.4, 1 mM EDTA, 150 mM NaCl, 1% NP-40, 0.25% Na-deoxycholate, and 1 μg/ml of aprotinin, leupeptin, and pepstatin). Equal amounts of protein (20 μg/sample) were separated by the NuPAGE Bis - Tris electrophoresis system (Invitrogen, Carlsbad, CA) and blotted onto nitrocellulose membrane (Whatman, Dassel, Germany). Blots were probed with primary and then secondary antibodies before exposure to Hyperfilm (Amersham Pharmacia Biotech).

Polyclonal antibody specific to AIF (SC-5586) and monoclonal antibodies specific for cytochrome c (SC-13156) and β-actin (SC-47778) were purchased from Santa Cruz Biotechnology (Santa Cruz, CA). Bcl-2 (2876), Bcl-xL (2762), Bid (2003), COX IV (4850), p-p53 (Ser 15)(9284), caspase-8 (4927), cleaved caspase-9 (Asp 353) (9509), cleaved caspase-3 (Asp 175) (9661), and cleaved caspase-7 (Asp 198) (9491) polyclonal antibodies were purchased from Cell Signaling (Beverly, MA). The monoclonal antibody specific to p53 (OP03), GAPDH (A00839-40), and Smac/Diablo (612245) were purchased from Oncogene, Genscript, and BD Bioscience (Pharmingen), respectively. The PARP (SA-249) antibody was purchased from Biomol. Secondary antibodies and enhanced chemiluminescence substrate were from Pierce (Rockford, IL).

Preparation of mitochondrial and cytosolic lysates

JB6 Cl4 cells were washed with PBS, resuspended in an ice-cold lysis buffer (250 mM sucrose, 20 mM *N*-(2-hydroxyethyl) piperazine-*N*′-(2-ethanesulfonic acid) (HEPES), pH 7.5, 10 mM KCl, 1.5 mM $MgCl_2$, 1 mM each of EGTA, EDTA, DTT and PMSF, and 10 μg/ml each of leupeptin, aprotinin and pepstatin A) and incubated for 20 min. The cells were centrifuged at 750 × *g* for 10 min at 4 °C, and the supernatants were further centrifuged at 10,000 × *g* for 25 min at 4 °C in order to prepare the cytosolic fraction. The remaining pellets were resuspended in the lysis buffer and used for mitochondrial fraction after centrifugation at 10,000 × *g* for 25 min.

Determination of caspase activity

The activity of caspases was assessed using the luminescent Caspase-Glo® 3/7 assay system (Promega, Madison, WI) according to the manufacturer's instructions. Briefly, cells were treated with various concentrations (0–10 μM) of Cr(VI) for 48 h and then 100 μl Caspase-

Glo® 3/7 Reagent was added into each 96-multiwell plates. After 1 h incubation at room temperature, the luminescence was measured using a Glomax™ 96 microplate luminometer (Promega, Madison, WI).

Measurement of mitochondrial membrane potential

The mitochondrial membrane potential (ΔΨm) was monitored using 5,5',6,6'-tetra-chloro-1,1',3,3'-tetraethylbenzimidazolyl-carbocyanine iodide (JC-1), a lipophilic cationic fluorescence dye. JC-1 is capable of selectively entering mitochondria, where it forms monomers, and emits green fluorescence (FL-1) when ΔΨm is relatively low. At a high ΔΨm, JC-1 aggregates and gives red fluorescence (FL-2) (Cossarizza et al., 1993). Thus the red and green fluorescence of JC-1 reflect the change of ΔΨm of the mitochondrial membrane. Briefly, cells (0.5×10^6 cells/well) were seeded into 60-mm culture dishes and treated with Cr(VI) (0–10 μM) for 48 h. Cells were trypsinized, washed in ice-cold PBS, and incubated with 2 μM JC-1 at 37 °C for 20 min. Finally, cells were washed twice with PBS and analyzed by flow cytometry.

Measurements of cellular hydrogen peroxide (H_2O_2) and superoxide anion ($O_2^{\bullet -}$) production

Dihydroethidium and CM-H_2DCFDA are specific dyes used for staining $O_2^{\bullet -}$ and H_2O_2, respectively, which are produced by intact cells (Qian et al., 2003; Zamzami et al., 1995). JB6 Cl41 cells (2×10^4 cells) were seeded onto a glass coverslide in the bottom of a 6-well plate overnight. The cells were exposed to Cr(V) (0–10 μM) for 24 h, and then dihydroethidium (5 μM) or CM-H_2DCFDA (5 μM) was added into the cells for 30 min. Cells were washed with PBS, mounted, and observed under an inverted confocal microscope (Leica, Wetzlar, Germany). In addition, JB6 Cl41 cells (0.5×10^6 cells/well) were seeded into 60-mm culture dishes before treating the cells with Cr(VI) (0–10 μM), CAT (500 U/ml) and/or SOD (500 U/ml) for 24 h. Finally, the cells were exposed to either dihydroethidium or CM-H_2DCFDA at a final concentration of 5 μM for 30 min and processed for flow cytometric analysis.

Electron spin resonance (ESR) assay

All ESR measurements were conducted using a Bruker EMX spectrometer (Bruker Instruments, Billerica, MA) and a flat cell assembly. A spin trap, 5,5-dimethyl-1-pyrroline-1-oxide (DMPO), was charcoal purified and distilled to remove all ESR detectable impurities before use. Hyperfine couplings were measured (to 0.1 G) directly from magnetic field separation using potassium tetraperoxochromate (K_3CrO_8) and 1,1-diphenyl-2-picrylhydrazyl (DPPH) as reference standards. The Acquisit program was used for data acquisitions and analyses (Bruker Instruments). Reactants were mixed in test tubes to a total final volume of 0.5 ml. The reaction mixture was then transferred to a flat cell for ESR measurement.

Small interfering RNA transfection

Silencer pre-designed small interference RNA (si-RNA) for mouse p53 (si-RNA ID: 187425) and control GAPDH (si-RNA ID: 4390849) were obtained from Ambion (Austin,

TX). JB6 Cl41 cells were seeded in 96- or 6-well culture plates and transfected at approximately 50% confluency with the si-RNA duplexes using Lipofectamine™ RNAi MAX (Invitrogen, Carlsbad, CA) according to the manufacturer's instructions. Medium was changed after 6 h to minimize cytotoxicity. Cellular levels of the proteins specific for the si-RNA transfection were checked by immunoblotting, and all experiments were performed 24 h after transfection.

Statistical analysis

All the data are expressed as mean ± standard error (SE). One-way analysis of variance (ANOVA) using SPSS ver. 10.0 software was used for multiple comparisons. A value of $P < 0.05$ was considered statistically significant.

Results

Cr(VI) induces cell death mainly by apoptosis in JB6 Cl41 cells in a dose-dependent manner

Cr(VI) induced a dose-dependent cytotoxic effect on JB6 Cl41 cells. Treatment of the cells with 1, 5, and 10 μM Cr(VI) for 48 h decreased the MTT-reducing activity to 89.2, 68.9, and 38.8%, respectively, relative to the untreated control cells (Fig. 1A). In addition, Cr(VI) significantly increased the number of trypan blue positive cells, such that approximately 67% of cells were positive to the dye when exposed to 10 μM Cr(VI) for 48 h (Fig. 1B). There was no cytotoxicity of cells under exposure to 1 μM Cr(VI). Cr(VI) treatment also caused cell death in a time-dependent manner (data not shown). Cr(VI)-induced toxicity was supported by optic microscopic observation, which showed an increase in cell shrinkage depending on the concentration of Cr(VI) (Fig. 1C).

The results from apoptosis assays revealed that Cr(VI)-induced cytotoxicity was due to apoptosis and necrosis (Fig. 2). Exposure of cells to Cr(VI) resulted in the increase of sub-G1 phage cells which mean apoptotic cells (Figs. 2A and 2B). When cells were exposed to 10 μM Cr(VI) for 48 h, approximately 40% of cell populations showed high FITC with low and/or high PI signals (Figs. 2C and 2D). These results support that Cr(VI) induced cell death is mainly due to apoptosis. This conclusion was also confirmed by the formation of genomic DNA ladders after Cr(VI) treatment (Fig. 2E).

Cr(VI)-induced apoptosis is mitochondria-mediated and caspase-dependent

Fig. 3A shows that Cr(VI) treatment activates executive caspases including caspase-3, -7, and -9 in JB6 cells. The chemical decreased cellular Bcl-2 and Bcl-xL levels. Degradation of procaspase-8 and cleavage of Bid and poly (ADP-ribose) polymerase (PARP) proteins were also observed when the cells were exposed to 10 μM Cr(VI). Further, treating the cells with Cr(VI) induced the release of cytochrome c and Smac/Diablo from the mitochondria (Fig. 3B). However, the levels of apoptosis-inducing factor (AIF) was not changed in either cytosolic or mitochondrial fraction of Cr(VI)-treated cells. These results suggest that Cr(VI) causes apoptosis through both mitochondrial-mediated and caspase-dependent pathways, whereas a well-known death effecter, AIF, is not associated with Cr(VI)-induced cell death.

In order to verify whether caspase cascade activation is involved in Cr(VI)-mediated apoptosis, the cells were incubated in combination with Cr(VI) (0–10 μM) and pancaspase inhibitor (Z-VAD, 20 μM). Activity of caspase 3/7 was significantly increased by treating cells with Cr(VI), which was completely diminished in the presence of Z-VAD fmk (Fig. 3C). Cr(VI)-induced increase apoptosis was also inhibited by adding Z-VAD into the cultures in a dose-dependent manner (Fig. 3D). In addition, flow cytometric analysis revealed that Cr(VI) decreased $\Delta\Psi m$ dramatically in JB6 cells (Figs. 4A and 4B). These results clarify that mitochondrial stress and caspase activation are involved in Cr(VI)-mediated apoptosis of JB6 Cl41 cells.

Intracellular production of ROS is important in Cr(VI)-induced cell death

Since accumulating evidence supports that intracellular ROS is produced by toxic chemicals and is participated in mediating cell signaling, we next determined whether Cr(VI) stimulates ROS generation in JB6 cells. Fluorescence intensities of DCF signals in the cells were right-shifted after Cr(VI) treatment in a dose-dependent manner (Fig. 5A). Similarly, fluorescence intensities of dihydroethidium were also increased by treating the cells with Cr(VI) (Fig. 5C). The Cr(VI)-stimulated DCF signal was apparently attenuated by adding catalase (CAT) into the cultures. Superoxide (SOD) treatment also diminished the fluorescence intensity specific for superoxide radical ($O_2^{\bullet -}$). The functions of CAT and SOD are to specifically scavenge hydrogen peroxide (H_2O_2) and $O_2^{\bullet -}$, respectively. These results indicate the Cr(VI) is able to generate intracellular ROS, H_2O_2 and $O_2^{\bullet -}$. These observations were supported by the fluorescence microscopic analyses showing that the cellular fluorescence specific for H_2O_2 (green color) and $O_2^{\bullet -}$ (red color) was increased by Cr(VI) treatment (Figs. 5B and 5D). Further, ESR spin trapping was used to detect free radical generation from Cr(VI)-stimulated JB6 cells. Fig. 5F shows the spectrum recorded from a mixture containing cells with or without Cr(VI) and CAT. As shown by this figure, cells alone did not generate any detectable ESR signal. Addition of Cr(VI) resulted in a generation of a 1:2:2:1 quartet ESR signal. The splittings of the spectrum were $a_H = a_N =$ 14.9 G, where a_H and a_N denote hyperfine splittings of the nitroxyl nitrogen and α-hydrogen, respectively. Based on these splittings and 1:2:2:1 line shape, this spectrum was assigned to the DMPO/$^{\bullet}$OH adduct (Shi and Dalal, 1989, 1990c), which is the evidence of $^{\bullet}$OH radical generation. Addition of CAT decreased the DMPO/$^{\bullet}$OH peak and generated a new one with g = 1.9785. Based on the previous studies, this new peak was assigned to Cr(V)-NADPH complex (Shi and Dalal, 1989, 1990c). The decrease of DMPO/$^{\bullet}$OH and generation of Cr(V)-NADPH upon addition of CAT indicate that Fenton type reaction [$Cr(V) + H_2O_2 \rightarrow Cr(VI) + {}^{\bullet}OH + OH^-$] is responsible for observed $^{\bullet}$OH radical generation. The Cr(V) and H_2O_2 are produced via cellular reduction of Cr(VI) (Ding and Shi, 2002; Shi and Dalal, 1989). Cr(VI)-induced decrease of cell viability was significantly prevented when the cells were treated with CAT or deferoxamine (DFX) (Fig. 5E). Treating the cells with sodium formate, a hydroxyl radical ($^{\bullet}$OH) scavenger, significantly attenuated the Cr(VI)-mediated cytotoxicity, indicating that $^{\bullet}$OH radical, the down stream of H_2O_2, is also involved in the overall mechanism of Cr(VI)-induced cell death. However, SOD treatment did not affect the Cr(VI)-induced reduction of cell viability in JB6 cells.

p53 activation is essential for Cr(VI)-induced cell death

Fig.5 shows the involvement of intracellular ROS generated by Cr(VI) in JB6 cells. Since ROS causes oxidative stress and eventually cell death, where p53-mediated signaling is involved, we investigated the effect of Cr(VI) on p53 phosphorylation in the cells. Western blot analysis reveals that treating JB6 cells with Cr(VI) increased the level of p-p53 in a dose- and time-dependent manner (Figs. 6A and 6B). The increase of p53 phosphorylation was started from 1 h and reached to maximum level after 24 h Cr(VI) treatment.

We further examined the roles of p53 in Cr(VI)-induced cell death by inhibiting its expressions with si-RNA transfection. The si-p53 transfection reduced the level of p-p53 increased by Cr(VI) to the basal level (Fig. 6C). The blockage of p53 significantly inhibited the Cr(VI)-mediated decrease of cell viability (Fig. 6D). In addition, the si-p53 transfection decreased the number of cells stained positively with annexin V/PI (Figs. 7A and 7C) and the mitochondrial membrane depolarization that had increased after Cr(VI) treatment (10 μM) (Figs. 7B and 7D). These results strongly suggest that p53 plays critical roles in mediating apoptosis in Cr(VI)-exposed JB6 cells.

Cr(VI) induces apoptosis through ROS-mediated p53 signaling in JB6 Cl41 cells

To further understand the signal transduction pathways involved in Cr(VI)-induced apoptosis, JB6 Cl41 cells were exposed to 10 μM Cr(VI) in the presence and absence of 500 U/ml CAT. Treating the cells with CAT decreased the level of p-p53 increased by Cr(VI) (Fig. 8A). The Cr(VI)-mediated events including the degradation of Bcl-2/Bcl-xL and procaspase-8 proteins, the increase of cleaved Bid and PARP proteins, and the activation of caspases-3, -7 and -9, were apparently blocked in the presence of CAT (Fig. 8A). Similarly, inhibition of p53 by its siRNA transfection suppressed the changes of Bcl-2 family proteins, caspases activation, and PARP cleavage that had stimulated after Cr(VI) exposure (Fig. 8B). These findings suggest that p53-mediated signaling plays pivotal role in Cr(VI)-induced apoptosis, where ROS act as upstream effecter.

Discussion

Cr(VI) affects a diverse range of cellular events such as proliferation, differentiation, and apoptosis. Whereas the cytotoxic and carcinogenic roles of Cr(VI) in the lung, liver, and kidney have been extensively studied, only limited studies are available for the skin. The selected doses which were used in our experiments came from *in vivo* data reported by Tsuneta et al. (Tsuneta et al., 1980) or Raithel et al.(Raithel et al., 1993). They found that the mean Cr content in the peripheral lung tissue in chromate workers was micromolar concentrations (30–100 μM). However, in certain occupational settings, chromate workers contained millimolar concentration of Cr in the lung (Ishikawa et al., 1994a, b). But they are exposed by chromate for a long time. Thus, the concentrations (1–10 μM) we used in this study are relevant to occupational exposure. Here we demonstrate that Cr(VI) induced cell death of JB6 Cl41 cells mainly by apoptosis through mitochondria-mediated and caspase-dependent pathways, where ROS-mediated p53 activation acted as upstream signaling.

Biochemical changes such as the activation of caspases and/or endonucleases are important characteristics in the process of typical apoptosis induction (Arends et al., 1990; Patel et al., 1996). Caspase-3 is a key apoptotic executive caspases, being activated by proteolytic cleavage due to caspase-8 and caspase-9 (Annunziato et al., 2003; Qu and Qing, 2004; Son et al., 2006a; Son et al., 2006b). Although some papers had reported that Cr(VI) induces apoptosis in lung epithelial cells, Chinese hamster ovary (CHO) cells, and lymphoma cells, it was not classified as either caspase-dependent or caspase-independent (Hayashi et al., 2004; Shimada et al., 1998; Ye et al., 1999). Our data reveal that caspase-dependent pathway is involved in the Cr(VI)-induced apoptosis. Actually, caspase cascade activation was apparent in the Cr(VI)-exposed cells. The cleavage of PARP, which is mediated by the activation of executive caspases (Annunziato et al., 2003; Yakovlev et al., 2000), was also observed in the cells. Furthermore, pancaspase inhibitor protected cells from Cr(VI)-mediated toxicity, thereby supporting the involvement of caspase-dependent signaling. However, recently Wang et.al. reported that Cr(VI) induced caspase-independent apoptosis in astrocytes (Wang et al., 2009). It is possible that different types of cells respond differently to apoptotic signaling.

Mitochondria play an important role in apoptosis induced both by caspase-dependent and -independent pathways. Bcl-2 and Bcl-xL are the major anti-apoptotic proteins integrated in mitochondrial membrane. These proteins prevent apoptosis through either hetero-dimerization with pro-apoptotic proteins, or their direct pore-forming effects on the outer membrane of mitochondria (Gross et al., 1999a; Harris and Thompson, 2000; Nechushtan et al., 2001). A notable result of this study is that that Cr(VI) reduces the cellular levels of antiapoptotic Bcl-2 family such as Bcl-2 and Bcl-xL in JB6 Cl41 cells, indicating the involvement of mitochondrial stress in Cr(VI)-induced apoptosis. It is worthwhile to consider that caspase-8 stimulates both caspase-dependent and -independent pathways by converting Bid to tBid (Gross et al., 1999b; Li et al., 1998; Yin et al., 1999). Production of tBid could induce mitochondrial stress, and also participate in the release of cytochrome c into cytosol. These lead us to suggest that caspase-8-Bid- and Bcl-2/Bcl-xL-mediated mitochondrial stress with the subsequent release of cytochrome c followed by caspase cascade activation are the executive mechanisms involved in Cr(VI)-mediated apoptosis (Fig. 9).

Although our previous studies, as well as those by other groups, have shown that Cr(VI) leads to the generation of ROS such as $^{\bullet}OH$, $O_2^{\bullet-}$, and H_2O_2 (Bagchi et al., 2001; Ding and Shi, 2002; Wang et al., 2000), this study showed that ROS was detected at a low concentration of Cr(VI) (10 μM) in a cellular system and antioxidant enzymes could suppress Cr(VI)-induced cytotoxicity. Moreover, treating cells with CAT prevented p53 phosphorylation, caspase activation, Bid cleavage, Bcl-2/Bcl-xL degradation, and PARP cleavage those had increased after Cr(VI) exposure. In contrast, SOD did not protect cells from Cr(VI)-mediated toxicity, despite of $O_2^{\bullet-}$ prominent generation after Cr(VI) treatment. SOD also did not inhibit Cr(VI)-induced phosphorylation of p53 and Bcl-2/Bcl-xL degradation (data not shown), whereas DFX showed a significant inhibition of Cr(VI)-induced cell death. This means that Cr(VI) stimulates the generation of both $O_2^{\bullet-}$ and H_2O_2 in JB6 cells, whereas H_2O_2 but not $O_2^{\bullet-}$ causes oxidative damage to the cells. It has been noted that among ROS, $^{\bullet}OH$ is the most toxic radical and can kill cells directly (Barbouti et

al., 2002; Lee et al., 2006; Wang et al., 2000). We observed that •OH was generated in Cr(VI)-exposed JB6 cells, and this effect was completely abrogated by the addition of CAT. $O_2^{\bullet-}$ is required for the generation of H_2O_2 through the enzymatic dismutation reaction of SOD (Shi and Dalal, 1992; Wang et al., 2000; Yao et al., 2008). Cr(VI) generates ROS via its reduction and/or a reaction with cellular small molecules such as glutathione (Shi and Dalal, 1990a; Shi and Dalal, 1988, 1990b). Cr(VI) also generates ROS through NAD(P)H oxidase activation (Shi and Dalal, 1989, 1990d; Wang et al., 2000). Moreover, we previously reported that Cr(VI) is able to generate •OH both by Haber-Weiss- and Fenton-like reactions (Ding and Shi, 2002; Liu et al., 1997; Shi and Dalal, 1992; Yao et al., 2008). Thus, in the cellular reduction of Cr(VI), a whole spectrum of ROS ($O_2^{\bullet-}$, H_2O_2 and •OH) is produced. In the present study, we have shown that SOD, the scavenger of $O_2^{\bullet-}$ radical, did not protect the Cr(VI)-induced cell death, indicating that $O_2^{\bullet-}$ is not directly involved in the Cr(VI)-involved cell death process. In stead, both CAT (the scavenger of H_2O_2) and sodium format (the scavenger of •OH) protected the cell death although at a different degree. These results demonstrate both H_2O_2 and •OH are involved in Cr(VI)-induced cell death. With these regards, it is suggested that •OH, which is produced from H_2O_2 by Fenton-like reaction, is a direct mediator of cell death in Cr(VI)-exposed JB6 cells, where $O_2^{\bullet-}$ may participate both in the production of H_2O_2 and in part the conversion of H_2O_2 to •OH by Haber-Weiss-like reaction.

p53 is an important regulator for apoptosis induced by ROS (Polyak et al., 1997; Tsang et al., 2003). There is a closed relationship among ROS, DNA damage and p53 activation. According to the conditions of DNA damage caused by ROS, the pattern of p53 expression can be differently affected, where a prolonged and persistent activation of p53 could lead to death signaling through changes of Bcl-2 protein family (Galluzzi et al., 2008; Kook et al., 2007; Lee et al., 2008). Cr(VI) can induce both p53-dependent (Carlisle et al., 2000; Wang et al., 2000; Ye et al., 1999) and p53-independent (Hayashi et al., 2004; Pritchard et al., 2000) apoptosis depending on the cell type. This study showed that Cr(VI) induces p53-dependent apoptosis in JB6 cells, because blockage of p53 expression with siRNA transfection dramatically prevented Cr(VI)-induced cytotoxicity, caspase activation, and mitochondrial membrane depolarization with the attendant increase of Bcl-2 and Bcl-xL expression. Collectively, our current data suggest that Cr(VI)-mediated ROS generation induced p53 phosphorylation, which signaled to the induction of apoptosis through caspase-dependent and mitochondrial-mediated pathways in JB6 cells.

In summary, this study demonstrates that Cr(VI) induces apoptosis predominently through caspase-dependent and mitochondria-mediated pathways, where ROS-mediated p53 activation is essential event. Many studies have been implicated the cellular mechanisms involved in Cr(VI)-mediated toxicity, and in the most cases, our current data are in parallel with previous reports (Bagchi et al., 2001; Carlisle et al., 2000; Hayashi et al., 2004; Pritchard et al., 2001; Singh et al., 1998). Here we further clarify the cellular mechanisms by which Cr(VI) causes apoptosis in skin epidermal cells, indicating that antioxidants can be applicable to protect the skin from Cr(VI)-induced toxic phenomenon. However, blockage of p53 by siRNA transfection or inhibition of caspase activity did not lead to a complete prevention on the Cr(VI)-mediated toxicity. These suggest that in addition to p53, other

mediators can be participated in inducing apoptosis of Cr(VI)-exposed cells. We are under investigating JNK signaling pathways in Cr(VI)-exposed cell death.

Acknowledgments

This research was supported by NIH grants (R01ES015518, 1R01CA119028, R01ES015375, and 1R01CA116697).

Abbreviations

MTT	3-(4,5-dimethylthiazol-2yl-)-2,5-diphenyl tetrazolium bromide
ROS	reactive oxygen species
CAT	catalase
SOD	superoxide dismutase
CM-H_2DCFDA	5-(and-6)-chloromethyl-2',7'-dichlorodihydrofluorescein diacetate
PI	propidium iodide
MMP	mitochondrial membrane potential
AIF	apoptosis-inducing factor
DAPI	4`-6-diamidino-2-phenylindole
PARP	poly (ADP-ribose) polymerase
JC-1	5,5',6,6'-tetra-chloro-1,1',3,3'-tetraethylbenzimidazolyl-carbocyanine iodide
4HPR	*N*-(4-hydroxyphenyl) retinamide
DMPO	5,5-dimethyl-1-pyrroline-1-oxide
DFX	deferoxamine
SF	sodium formate
ESR	electron spin resonance
Cr(VI)	hexavalent chromium
Cr(III)	trivalent chromium
Cr(V)	pentavalent chromium
Cr(IV)	tetravalent chromium

References

Annunziato L, Amoroso S, Pannaccione A, Cataldi M, Pignataro G, D'Alessio A, Sirabella R, Secondo A, Sibaud L, Di Renzo GF. Apoptosis induced in neuronal cells by oxidative stress: role played by caspases and intracellular calcium ions. Toxicol Lett. 2003; 139:125–133. [PubMed: 12628748]

Arends MJ, Morris RG, Wyllie AH. Apoptosis. The role of the endonuclease. Am J Pathol. 1990; 136:593–608. [PubMed: 2156431]

Bagchi D, Bagchi M, Stohs SJ. Chromium (VI)-induced oxidative stress, apoptotic cell death and modulation of p53 tumor suppressor gene. Mol Cell Biochem. 2001; 222:149–158. [PubMed: 11678597]

Barbouti A, Amorgianiotis C, Kolettas E, Kanavaros P, Galaris D. Hydrogen peroxide inhibits caspase-dependent apoptosis by inactivating procaspase-9 in an iron-dependent manner. Free Radic Biol Med. 2007; 43:1377–1387. [PubMed: 17936184]

Barbouti A, Doulias PT, Nousis L, Tenopoulou M, Galaris D. DNA damage and apoptosis in hydrogen peroxide-exposed Jurkat cells: bolus addition versus continuous generation of H(2)O(2). Free Radic Biol Med. 2002; 33:691–702. [PubMed: 12208356]

Blankenship LJ, Manning FC, Orenstein JM, Patierno SR. Apoptosis is the mode of cell death caused by carcinogenic chromium. Toxicol Appl Pharmacol. 1994; 126:75–83. [PubMed: 8184436]

Carlisle DL, Pritchard DE, Singh J, Owens BM, Blankenship LJ, Orenstein JM, Patierno SR. Apoptosis and P53 induction in human lung fibroblasts exposed to chromium (VI): effect of ascorbate and tocopherol. Toxicol Sci. 2000; 55:60–68. [PubMed: 10788560]

Cohen MD, Kargacin B, Klein CB, Costa M. Mechanisms of chromium carcinogenicity and toxicity. Crit Rev Toxicol. 1993; 23:255–281. [PubMed: 8260068]

Connett P, Wetterhahn K. Metabolism of the carcinogenic chromate by cellular constituents. Struct Bonding. 1983; 54:93–124.

Cossarizza A, Baccarani-Contri M, Kalashnikova G, Franceschi C. A new method for the cytofluorimetric analysis of mitochondrial membrane potential using the J-aggregate forming lipophilic cation 5,5',6,6'-tetrachloro-1,1',3,3'-tetraethylbenzimidazolcarbocyanine iodide (JC-1). Biochem Biophys Res Commun. 1993; 197:40–45. [PubMed: 8250945]

Costa M. Toxicity and carcinogenicity of Cr(VI) in animal models and humans. Crit Rev Toxicol. 1997; 27:431–442. [PubMed: 9347224]

D'Agostini F, Izzotti A, Bennicelli C, Camoirano A, Tampa E, De Flora S. Induction of apoptosis in the lung but not in the liver of rats receiving intra-tracheal instillations of chromium(VI). Carcinogenesis. 2002; 23:587–593. [PubMed: 11960910]

Ding M, Shi X. Molecular mechanisms of Cr(VI)-induced carcinogenesis. Mol Cell Biochem. 2002; 234–235:293–300.

Flores A, Perez JM. Cytotoxicity, apoptosis, and in vitro DNA damage induced by potassium chromate. Toxicol Appl Pharmacol. 1999; 161:75–81. [PubMed: 10558925]

Galluzzi L, Morselli E, Kepp O, Tajeddine N, Kroemer G. Targeting p53 to mitochondria for cancer therapy. Cell Cycle. 2008; 7:1949–1955. [PubMed: 18642442]

Ghelli A, Zanna C, Porcelli AM, Schapira AH, Martinuzzi A, Carelli V, Rugolo M. Leber's hereditary optic neuropathy (LHON) pathogenic mutations induce mitochondrial-dependent apoptotic death in transmitochondrial cells incubated with galactose medium. J Biol Chem. 2003; 278:4145–4150. [PubMed: 12446713]

Gross A, McDonnell JM, Korsmeyer SJ. BCL-2 family members and the mitochondria in apoptosis. Genes Dev. 1999a; 13:1899–1911. [PubMed: 10444588]

Gross A, Yin XM, Wang K, Wei MC, Jockel J, Milliman C, Erdjument-Bromage H, Tempst P, Korsmeyer SJ. Caspase cleaved BID targets mitochondria and is required for cytochrome c release, while BCL-XL prevents this release but not tumor necrosis factor-R1/Fas death. J Biol Chem. 1999b; 274:1156–1163. [PubMed: 9873064]

Hansen MB, Menne T, Johansen JD. Cr(III) and Cr(VI) in leather and elicitation of eczema. Contact Dermatitis. 2006; 54:278–282. [PubMed: 16689813]

Harris MH, Thompson CB. The role of the Bcl-2 family in the regulation of outer mitochondrial membrane permeability. Cell Death Differ. 2000; 7:1182–1191. [PubMed: 11175255]

Hayashi Y, Kondo T, Zhao QL, Ogawa R, Cui ZG, Feril LB Jr, Teranishi H, Kasuya M. Signal transduction of p53-independent apoptotic pathway induced by hexavalent chromium in U937 cells. Toxicol Appl Pharmacol. 2004; 197:96–106. [PubMed: 15163545]

Hodges NJ, Adam B, Lee AJ, Cross HJ, Chipman JK. Induction of DNA-strand breaks in human peripheral blood lymphocytes and A549 lung cells by sodium dichromate: association with 8-oxo-2-deoxyguanosine formation and inter-individual variability. Mutagenesis. 2001; 16:467–474. [PubMed: 11682636]

Ishikawa Y, Nakagawa K, Satoh Y, Kitagawa T, Sugano H, Hirano T, Tsuchiya E. Characteristics of chromate workers' cancers, chromium lung deposition and precancerous bronchial lesions: an autopsy study. Br J Cancer. 1994a; 70:160–166. [PubMed: 8018529]

Ishikawa Y, Nakagawa K, Satoh Y, Kitagawa T, Sugano H, Hirano T, Tsuchiya E. "Hot spots" of chromium accumulation at bifurcations of chromate workers' bronchi. Cancer Res. 1994b; 54:2342–2346. [PubMed: 8162579]

Joseph P, He Q, Umbright C. Heme-oxygenase 1 gene expression is a marker for hexavalent chromium-induced stress and toxicity in human dermal fibroblasts. Toxicol Sci. 2008; 103:325–334. [PubMed: 18332044]

Kook SH, Son YO, Chung SW, Lee SA, Kim JG, Jeon YM, Lee JC. Caspase-independent death of human osteosarcoma cells by flavonoids is driven by p53-mediated mitochondrial stress and nuclear translocation of AIF and endonuclease G. Apoptosis. 2007; 12:1289–1298. [PubMed: 17356895]

Kroemer G, Reed JC. Mitochondrial control of cell death. Nat Med. 2000; 6:513–519. [PubMed: 10802706]

Lee JC, Son YO, Choi KC, Jang YS. Hydrogen peroxide induces apoptosis of BJAB cells due to formation of hydroxyl radicals via intracellular iron-mediated Fenton chemistry in glucose oxidase-mediated oxidative stress. Mol Cells. 2006; 22:21–29. [PubMed: 16951546]

Lee KB, Kim KR, Huh TL, Lee YM. Proton induces apoptosis of hypoxic tumor cells by the p53-dependent and p38/JNK MAPK signaling pathways. Int J Oncol. 2008; 33:1247–1256. [PubMed: 19020758]

Li H, Zhu H, Xu CJ, Yuan J. Cleavage of BID by caspase 8 mediates the mitochondrial damage in the Fas pathway of apoptosis. Cell. 1998; 94:491–501. [PubMed: 9727492]

Li P, Nijhawan D, Budihardjo I, Srinivasula SM, Ahmad M, Alnemri ES, Wang X. Cytochrome c and dATP-dependent formation of Apaf-1/caspase-9 complex initiates an apoptotic protease cascade. Cell. 1997; 91:479–489. [PubMed: 9390557]

Liu KJ, Shi X, Dalal NS. Synthesis of Cr(IV)-GSH, its identification and its free hydroxyl radical generation: a model compound for Cr(VI) carcinogenicity. Biochem Biophys Res Commun. 1997; 235:54–58. [PubMed: 9196034]

Nechushtan A, Smith CL, Lamensdorf I, Yoon SH, Youle RJ. Bax and Bak coalesce into novel mitochondria-associated clusters during apoptosis. J Cell Biol. 2001; 153:1265–1276. [PubMed: 11402069]

Patel T, Gores GJ, Kaufmann SH. The role of proteases during apoptosis. FASEB J. 1996; 10:587–597. [PubMed: 8621058]

Polyak K, Xia Y, Zweier JL, Kinzler KW, Vogelstein B. A model for p53-induced apoptosis. Nature. 1997; 389:300–305. [PubMed: 9305847]

Pritchard DE, Ceryak S, Ha L, Fornsaglio JL, Hartman SK, O'Brien TJ, Patierno SR. Mechanism of apoptosis and determination of cellular fate in chromium(VI)-exposed populations of telomerase-immortalized human fibroblasts. Cell Growth Differ. 2001; 12:487–496. [PubMed: 11682460]

Pritchard DE, Singh J, Carlisle DL, Patierno SR. Cyclosporin A inhibits chromium(VI)-induced apoptosis and mitochondrial cytochrome c release and restores clonogenic survival in CHO cells. Carcinogenesis. 2000; 21:2027–2033. [PubMed: 11062164]

Qian Y, Luo J, Leonard SS, Harris GK, Millecchia L, Flynn DC, Shi X. Hydrogen peroxide formation and actin filament reorganization by Cdc42 are essential for ethanol-induced in vitro angiogenesis. J Biol Chem. 2003; 278:16189–16197. [PubMed: 12598535]

Qu X, Qing L. Abrin induces HeLa cell apoptosis by cytochrome c release and caspase activation. J Biochem Mol Biol. 2004; 37:445–453. [PubMed: 15469732]

Raithel HJ, Schaller KH, Kraus T, Lehnert G. Biomonitoring of nickel and chromium in human pulmonary tissue. Int Arch Occup Environ Health. 1993; 65:S197–S200. [PubMed: 8406925]

Shelnutt SR, Goad P, Belsito DV. Dermatological toxicity of hexavalent chromium. Crit Rev Toxicol. 2007; 37:375–387. [PubMed: 17612952]

Shi X, Chiu A, Chen CT, Halliwell B, Castranova V, Vallyathan V. Reduction of chromium(VI) and its relationship to carcinogenesis. J Toxicol Environ Health B Crit Rev. 1999; 2:87–104. [PubMed: 10081526]

Shi XG, Dalal NS. On the hydroxyl radical formation in the reaction between hydrogen peroxide and biologically generated chromium(V) species. Arch Biochem Biophys. 1990a; 277:342–350. [PubMed: 2155579]

Shi XL, Dalal NS. On the mechanism of the chromate reduction by glutathione: ESR evidence for the glutathionyl radical and an isolable Cr(V) intermediate. Biochem Biophys Res Commun. 1988; 156:137–142. [PubMed: 2845969]

Shi XL, Dalal NS. Chromium (V) and hydroxyl radical formation during the glutathione reductase-catalyzed reduction of chromium (VI). Biochem Biophys Res Commun. 1989; 163:627–634. [PubMed: 2550002]

Shi XL, Dalal NS. ESR spin trapping detection of hydroxyl radicals in the reactions of Cr(V) complexes with hydrogen peroxide. Free Radic Res Commun. 1990b; 10:17–26. [PubMed: 2165982]

Shi XL, Dalal NS. Evidence for a Fenton-type mechanism for the generation of .OH radicals in the reduction of Cr(VI) in cellular media. Arch Biochem Biophys. 1990c; 281:90–95. [PubMed: 2166480]

Shi XL, Dalal NS. NADPH-dependent flavoenzymes catalyze one electron reduction of metal ions and molecular oxygen and generate hydroxyl radicals. FEBS Lett. 1990d; 276:189–191. [PubMed: 2176163]

Shi XL, Dalal NS. The role of superoxide radical in chromium (VI)-generated hydroxyl radical: the Cr(VI) Haber-Weiss cycle. Arch Biochem Biophys. 1992; 292:323–327. [PubMed: 1309299]

Shimada H, Shiao YH, Shibata M, Waalkes MP. Cadmium suppresses apoptosis induced by chromium. J Toxicol Environ Health A. 1998; 54:159–168. [PubMed: 9652551]

Singh J, Carlisle DL, Pritchard DE, Patierno SR. Chromium-induced genotoxicity and apoptosis: relationship to chromium carcinogenesis (review). Oncol Rep. 1998; 5:1307–1318. [PubMed: 9769362]

Son YO, Choi KC, Lee JC, Kook SH, Lee HJ, Jeon YM, Kim JG, Kim J, Lee WK, Jang YS. Involvement of caspase activation and mitochondrial stress in trichostatin A-induced apoptosis of Burkitt's lymphoma cell line, Akata. J Cell Biochem. 2006a; 99:1420–1430. [PubMed: 16817225]

Son YO, Choi KC, Lee JC, Kook SH, Lee SK, Takada K, Jang YS. Involvement of caspase activation and mitochondrial stress in taxol-induced apoptosis of Epstein-Barr virus-infected Akata cells. Biochim Biophys Acta. 2006b; 1760:1894–1902. [PubMed: 16938399]

Son YO, Jang YS, Heo JS, Chung WT, Choi KC, Lee JC. Apoptosis-inducing factor plays a critical role in caspase-independent, pyknotic cell death in hydrogen peroxide-exposed cells. Apoptosis. 2009a; 14:796–808. [PubMed: 19418225]

Son YO, Kook SH, Jang YS, Shi X, Lee JC. Critical role of poly(ADP-ribose) polymerase-1 in modulating the mode of cell death caused by continuous oxidative stress. J Cell Biochem. 2009b; 108:989–997. [PubMed: 19711368]

Stohs SJ, Bagchi D, Hassoun E, Bagchi M. Oxidative mechanisms in the toxicity of chromium and cadmium ions. J Environ Pathol Toxicol Oncol. 2000; 19:201–213. [PubMed: 10983887]

Susin SA, Lorenzo HK, Zamzami N, Marzo I, Brenner C, Larochette N, Prevost MC, Alzari PM, Kroemer G. Mitochondrial release of caspase-2 and-9 during the apoptotic process. J Exp Med. 1999; 189:381–394. [PubMed: 9892620]

Tsang WP, Chau SP, Kong SK, Fung KP, Kwok TT. Reactive oxygen species mediate doxorubicin induced p53-independent apoptosis. Life Sci. 2003; 73:2047–2058. [PubMed: 12899928]

Tsuneta Y, Ohsaki Y, Kimura K, Mikami H, Abe S, Murao M. Chromium content of lungs of chromate workers with lung cancer. Thorax. 1980; 35:294–297. [PubMed: 7434272]

Waalkes MP, Fox DA, States JC, Patierno SR, McCabe MJ Jr. Metals and disorders of cell accumulation: modulation of apoptosis and cell proliferation. Toxicol Sci. 2000; 56:255–261. [PubMed: 10910982]

Wang CC, Fang KM, Yang CS, Tzeng SF. Reactive oxygen species-induced cell death of rat primary astrocytes through mitochondria-mediated mechanism. J Cell Biochem. 2009; 107:933–943. [PubMed: 19459161]

Wang S, Leonard SS, Ye J, Ding M, Shi X. The role of hydroxyl radical as a messenger in Cr(VI)-induced p53 activation. Am J Physiol Cell Physiol. 2000; 279:C868–C875. [PubMed: 10942736]

Xu J, Wise JP, Patierno SR. DNA damage induced by carcinogenic lead chromate particles in cultured mammalian cells. Mutat Res. 1992; 280:129–136. [PubMed: 1378537]

Yakovlev AG, Wang G, Stoica BA, Boulares HA, Spoonde AY, Yoshihara K, Smulson ME. A role of the Ca2+/Mg2+-dependent endonuclease in apoptosis and its inhibition by Poly(ADP-ribose) polymerase. J Biol Chem. 2000; 275:21302–21308. [PubMed: 10807908]

Yao H, Guo L, Jiang BH, Luo J, Shi X. Oxidative stress and chromium(VI) carcinogenesis. J Environ Pathol Toxicol Oncol. 2008; 27:77–88. [PubMed: 18540844]

Ye J, Wang S, Leonard SS, Sun Y, Butterworth L, Antonini J, Ding M, Rojanasakul Y, Vallyathan V, Castranova V, Shi X. Role of reactive oxygen species and p53 in chromium(VI)-induced apoptosis. J Biol Chem. 1999; 274:34974–34980. [PubMed: 10574974]

Ye J, Zhang X, Young HA, Mao Y, Shi X. Chromium(VI)-induced nuclear factor-kappa B activation in intact cells via free radical reactions. Carcinogenesis. 1995; 16:2401–2405. [PubMed: 7586142]

Yin XM, Wang K, Gross A, Zhao Y, Zinkel S, Klocke B, Roth KA, Korsmeyer SJ. Bid-deficient mice are resistant to Fas-induced hepatocellular apoptosis. Nature. 1999; 400:886–891. [PubMed: 10476969]

Zamzami N, Marchetti P, Castedo M, Decaudin D, Macho A, Hirsch T, Susin SA, Petit PX, Mignotte B, Kroemer G. Sequential reduction of mitochondrial transmembrane potential and generation of reactive oxygen species in early programmed cell death. J Exp Med. 1995; 182:367–377. [PubMed: 7629499]

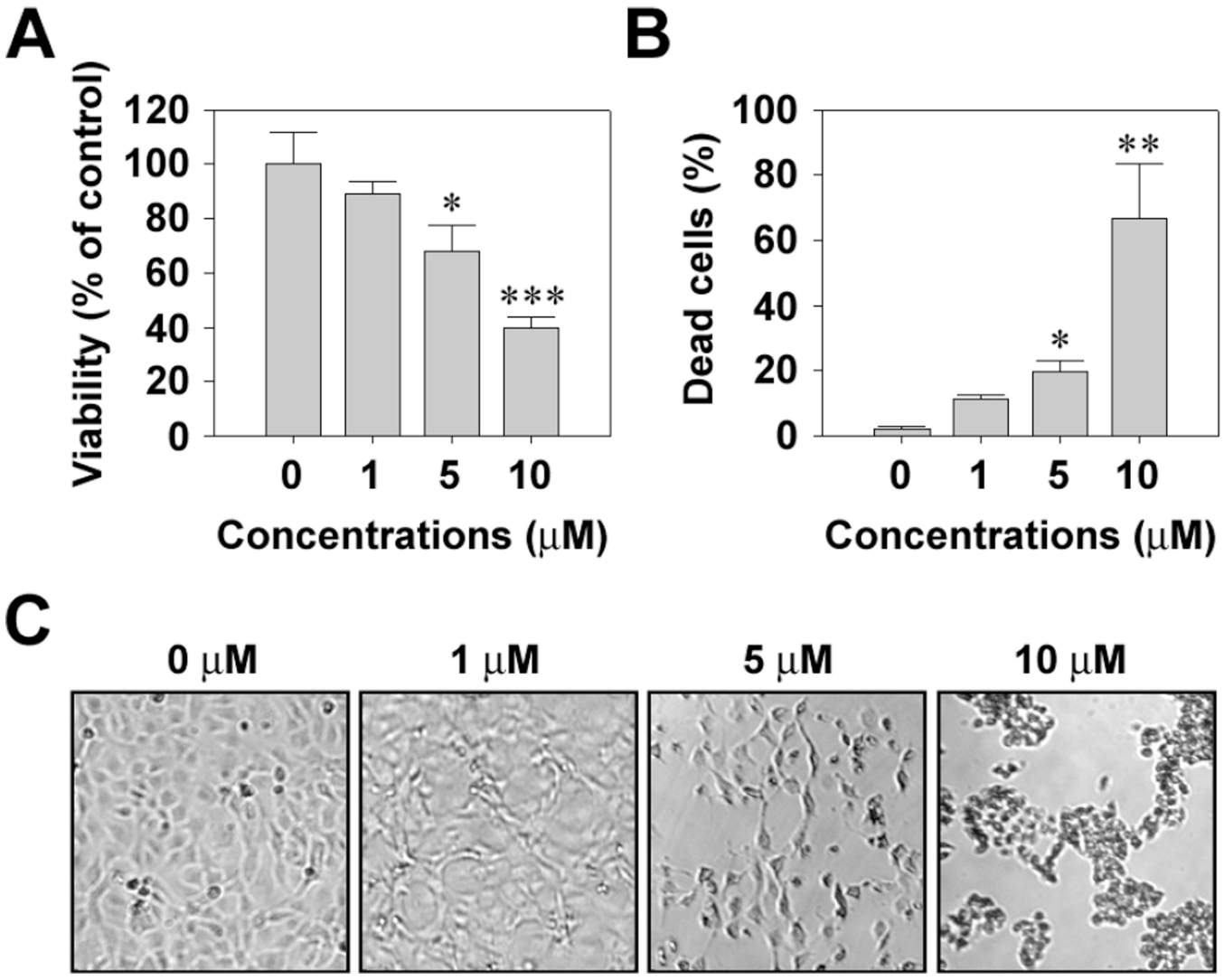

Fig. 1.

Cr(VI) induces cytotoxicity of JB6 cells in a dose-dependent manner. JB6 cells were incubated with Cr(VI) at the indicated concentrations for 48 h and then processed for MTT assay (A) and trypan blue staining (B). The results are shown as the mean ± SE of three separate experiments. $^{*}P < 0.05$, $^{**}P < 0.01$, and $^{***}P < 0.001$ vs. the control values (ANOVA, Scheffe's test). (C) Changes of cell morphology in Cr(VI)-exposed cells were also observed by optic microscope (magnification, ×40).

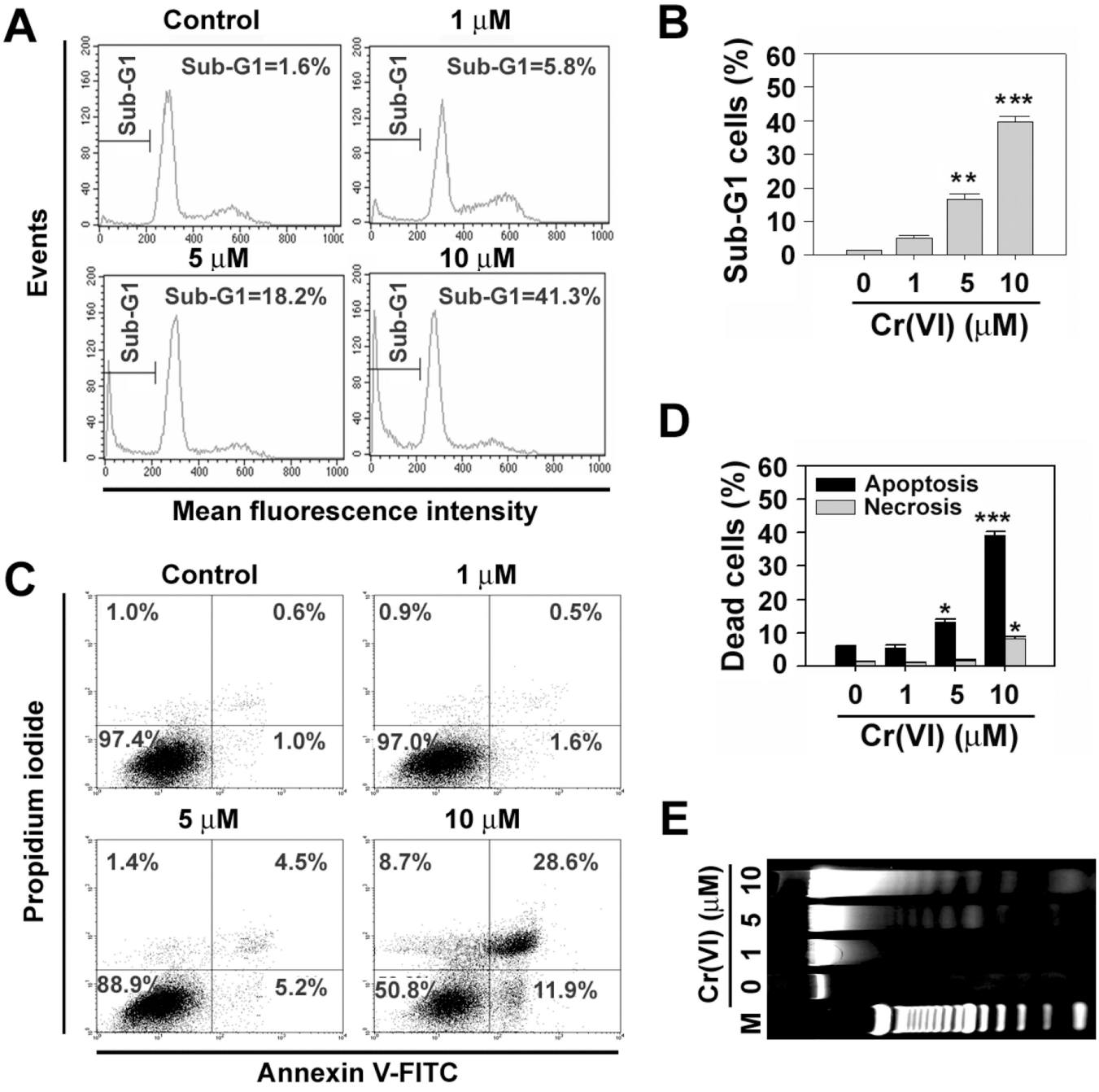

Fig. 2.

Cr(VI) induces apoptotic cell death in JB6 cells. JB6 cells were exposed to the increasing concentrations (0–10 μM) of Cr(VI). At 48 h of exposure, they were analyzed using flow cytometer after staining with PI (A) or annexin V and PI (C). The percentages of cell populations in the sub-G1 phase (B) and early and late apoptotic cells with annexin V^+/PI^- and annexin V^+/PI^+ (D) were calculated using WinMDI 2.9 program. (E) In addition, the cells were processed for the analysis of genomic DNA ladder formation. The results are shown as the mean ± SE of triplicate experiments. $^*P < 0.05$, $^{**}P < 0.01$, and $^{***}P < 0.001$ vs. control (ANOVA, Scheffe's test). In panel E, M means DNA size marker.

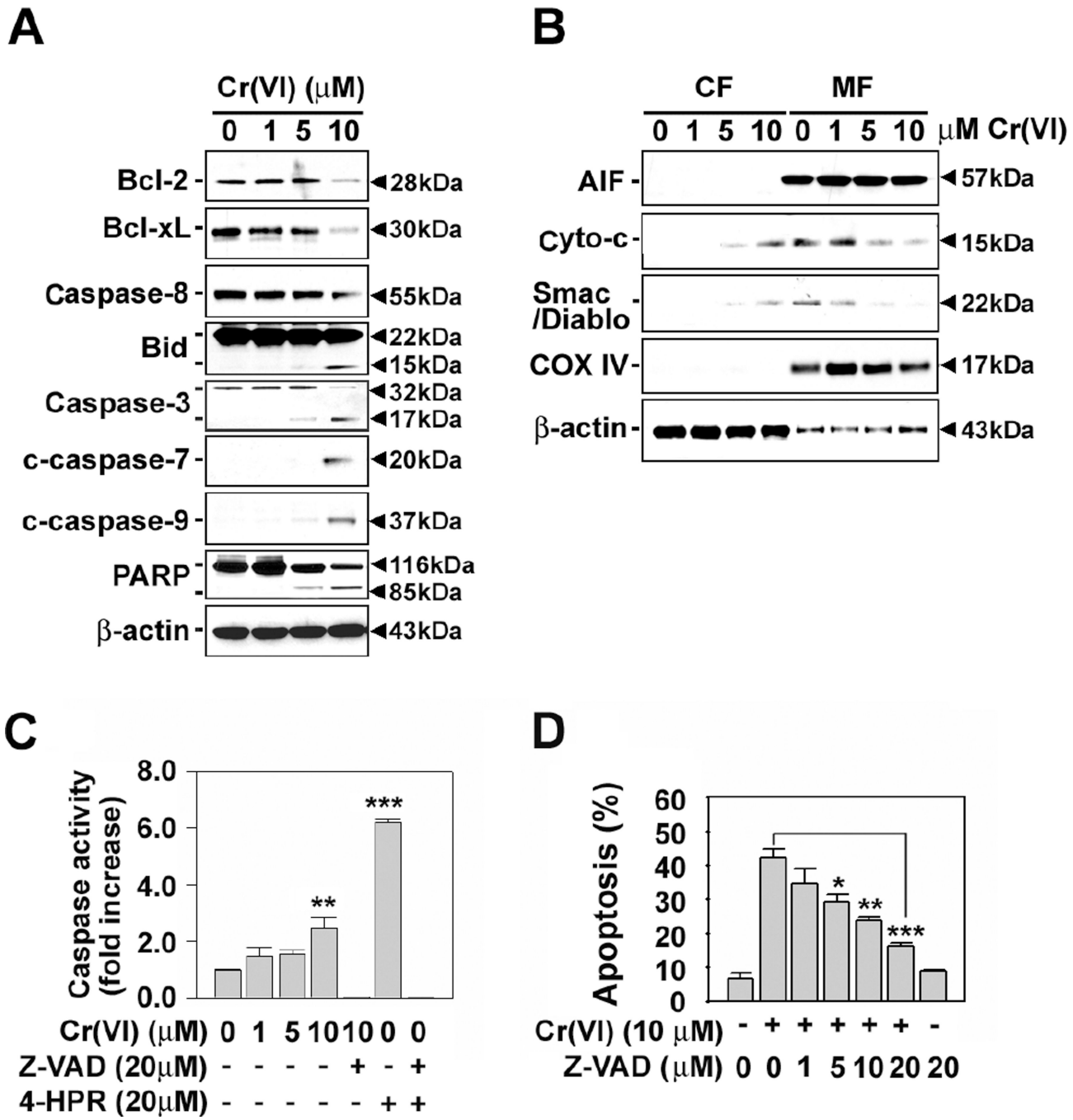

Fig. 3.

Effects of Cr(VI) on mitochondria apoptotic effectors and caspases in JB6 cells. Cells were incubated with Cr(VI) at the indicated concentrations for 48 h. (A) Whole cell lysates or (B) cytosolic and mitochondria fractions were analyzed by immunoblotting using various primary antibodies specific for mitochondria-related death molecules. Cytochrome c oxidase IV (COX IV) was used as internal marker specific to mitochondria. A representative result is shown from triplicate experiments. CF, cytosolic fraction. MF, mitochondrial fraction. Cells were incubated with Cr(VI) at the indicated concentration for 48 h in the presence and

absence of pancaspase inhibitor (Z-VAD, 20 μM) and/or 4-HPR (20 μM). Thereafter, caspase activity (C) and apoptosis (D) were determined using luminescent Caspase-Glo® 3/7 Assay system and annexin V/PI assay, respectively. Values are the means ± SE of three independent experiments. 4-HPR was used as a caspase-dependent positive control. $^{*}P < 0.05$, $^{**}P < 0.01$ and $^{***}P < 0.001$ vs. the control value or Cr(VI) treatment alone (ANOVA, Scheffe's test).

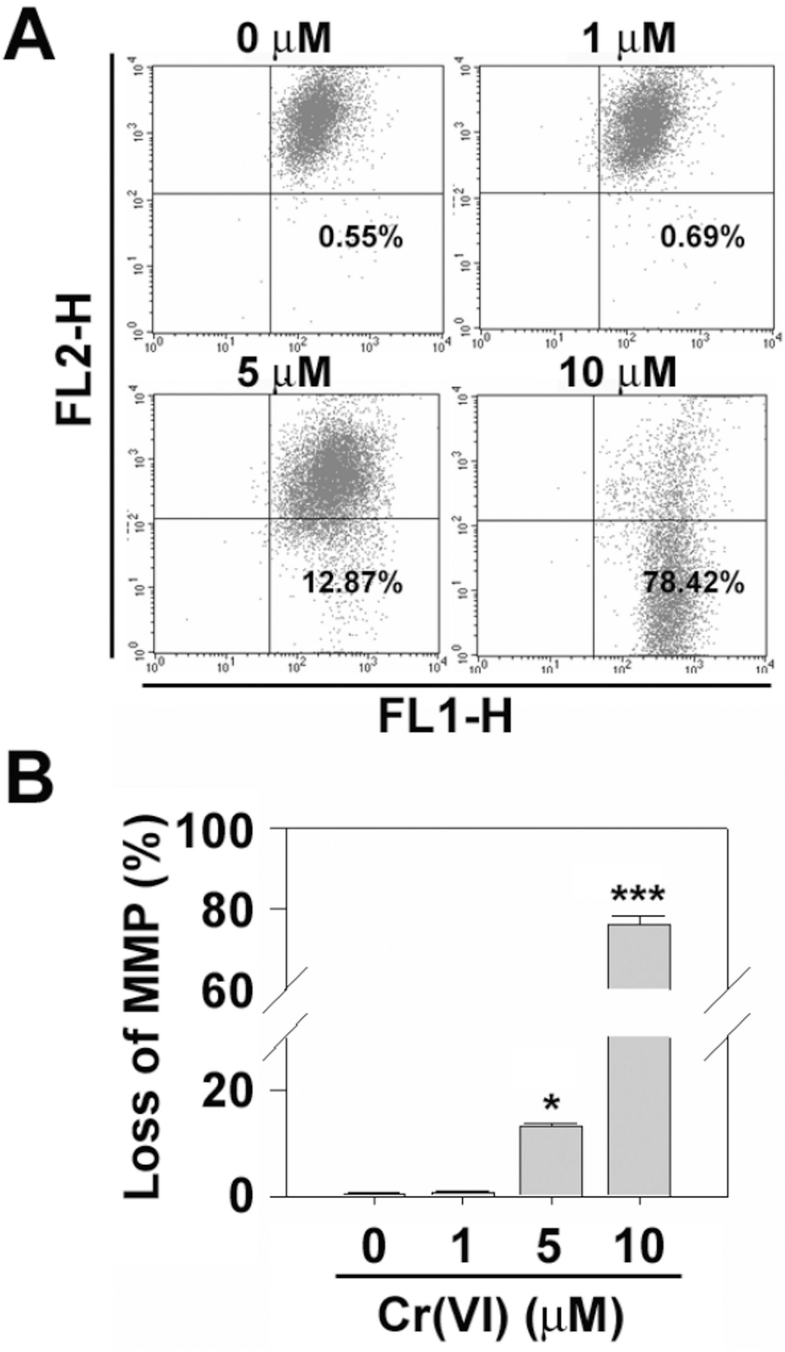

Fig. 4.

Cr(VI) induces mitochondrial stress in JB6 cells. (A) Cr(VI)-treated JB6 cells for 48 h were incubated with 2 μM JC-1 dye for 15 min, and the intensities of FL-1 and FL-2 fluorescence were measured by flow cytometer. (B) Percentages of depolarized populations were calculated, and the results are shown as the mean ± SE of triplicate experiments. $^{*}P < 0.05$ and $^{***}P < 0.001$ vs. the control value (ANOVA, Scheffe's test).

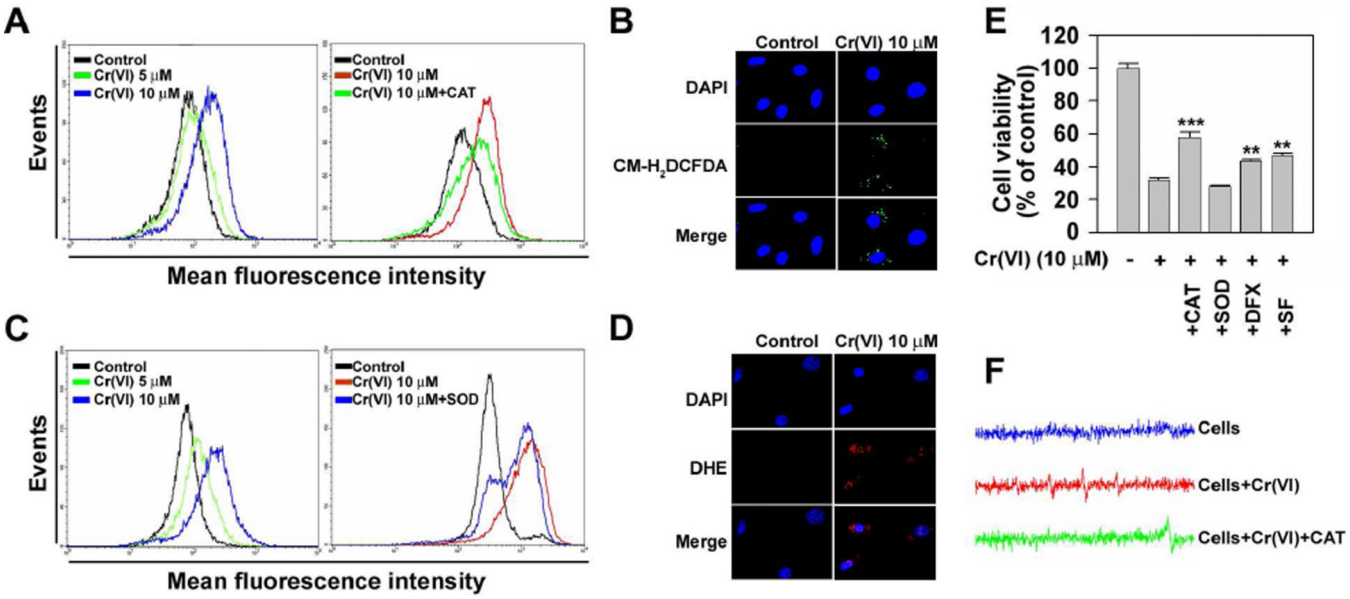

Fig. 5.

Cr(VI) causes cell death mainly through generation of ROS in JB6 cells. JB6 cells were incubated with various Cr(VI) concentrations (0–10 μM) for 24 h and then exposed to CM-H_2DCFDA (25 μM) (A) or dihydroethidium (10 μM) (C) for an additional 15 min prior to the analysis using flow cytometer. In addition, the cells were immediately stained with 2 μM CM-H_2DCFDA or 10 μM dihydroethidium before counterstaining with DAPI (4′,6-diamidino-2-phenylindole) (B and D) and then analyzed under fluorescence microscope (magnification, ×200). JB6 cells were incubated with 10 μM Cr(VI) in the presence and absence of CAT (500 U/ml), SOD (500 U/ml), DFX (100 μM) and/or SF (10 mM). After 48 h of incubation, the cells were processed for MTT assay (E). Results are shown as mean ± SE of three separate experiments. $^{**}P < 0.01$, and $^{***}P < 0.001$ vs. Cr(VI) treatment alone. (F) Electron spin resonance (ESR) spectrum recorded 15 min after the addition of 10 μM Cr(VI) to 2×10^6 cells and 100 mM 5,5-dimethyl-1-pyrroline 1-oxide with or without CAT (500 U/ml). CAT, catalase; SOD, superoxide dismutase; DFX, deferoxamine; SF, sodium formate.

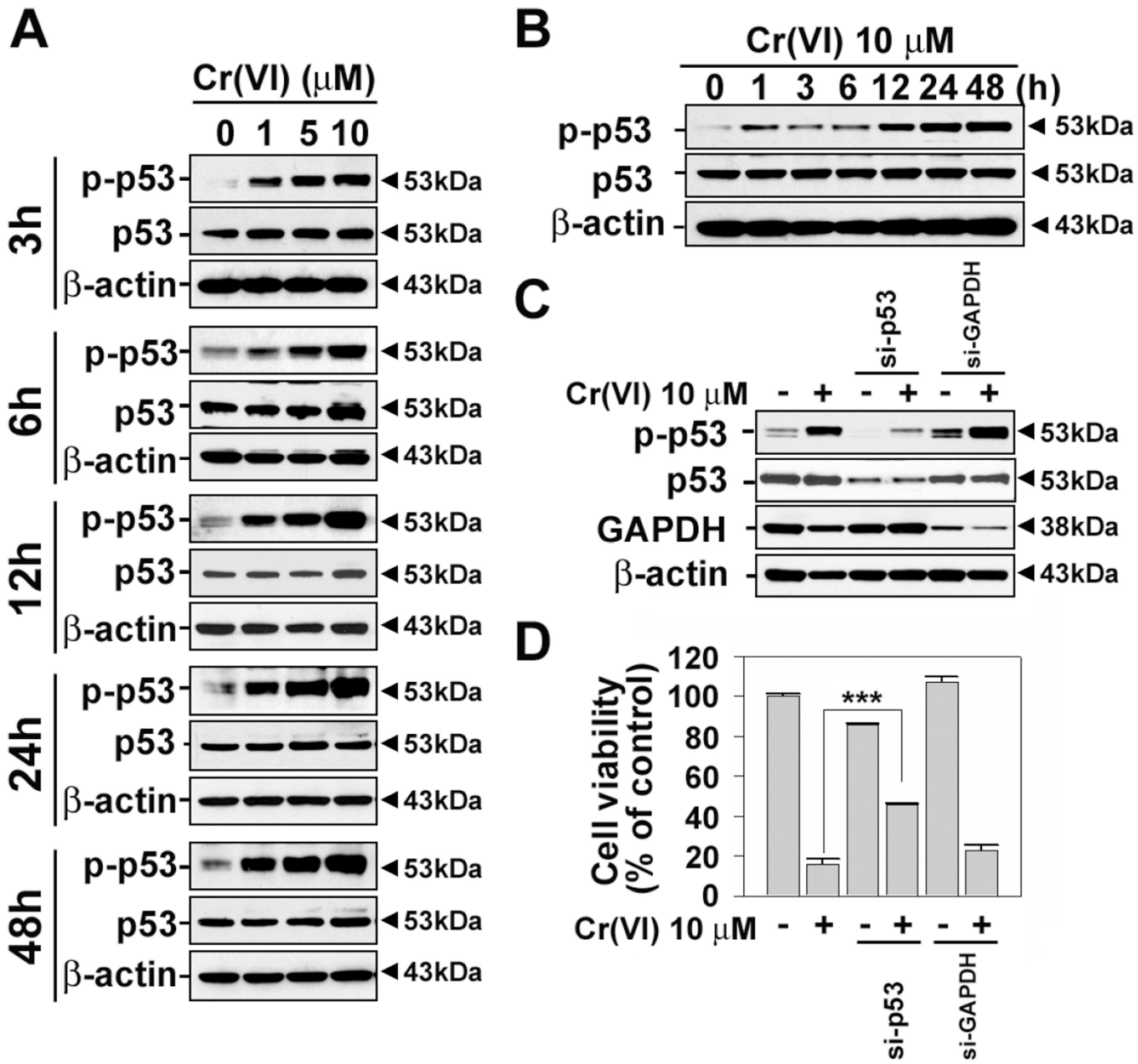

Fig. 6.

p53 phosphorylation is essential for Cr(VI)-induced cell death. JB6 cells were incubated with Cr(VI) at the various concentrations (0–10 μM) for various times (3–48 h) (A) or at 10 μM for various times (0–48 h) (B), and then the levels of p-p53 (ser 15) were analyzed by western blotting. JB6 cells were transfected with si-RNA specific to p53 or GAPDH, and after 24 h of transfection they were exposed to 10 μM Cr(VI) for additional 48 h. Thereafter, the cells were adjusted to the western blot analysis (C) and MTT assay (D). The results are shown as the mean ± SE of three separate experiments. $^{***}P < 0.001$ vs. the experiments.

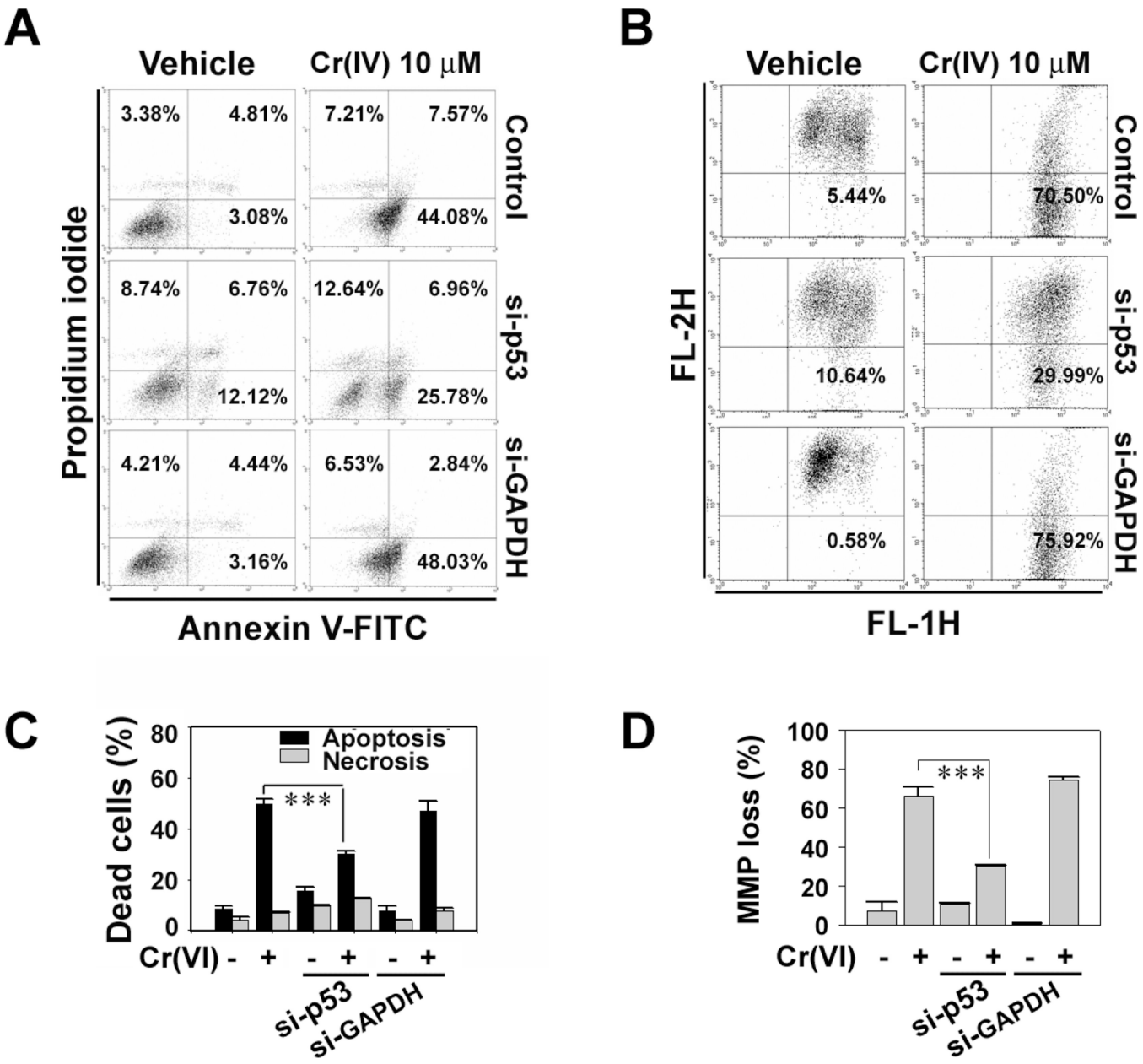

Fig. 7.

p53 is required for apoptosis and mitochondrial stress caused by Cr(VI) in JB6 cells. JB6 cells were transfected with si-RNA specific to p53 or GAPDH, and after 24 h of transfection they were exposed to 10 μM Cr(VI) for additional 48 h. The cells were performed flow cytometric analysis after annexin V/PI staining (A) or JC-1 dye staining (B). In the figures C and D, the results are shown as the mean ± SE of three separate experiments. $^{***}P < 0.001$ vs. the experiments.

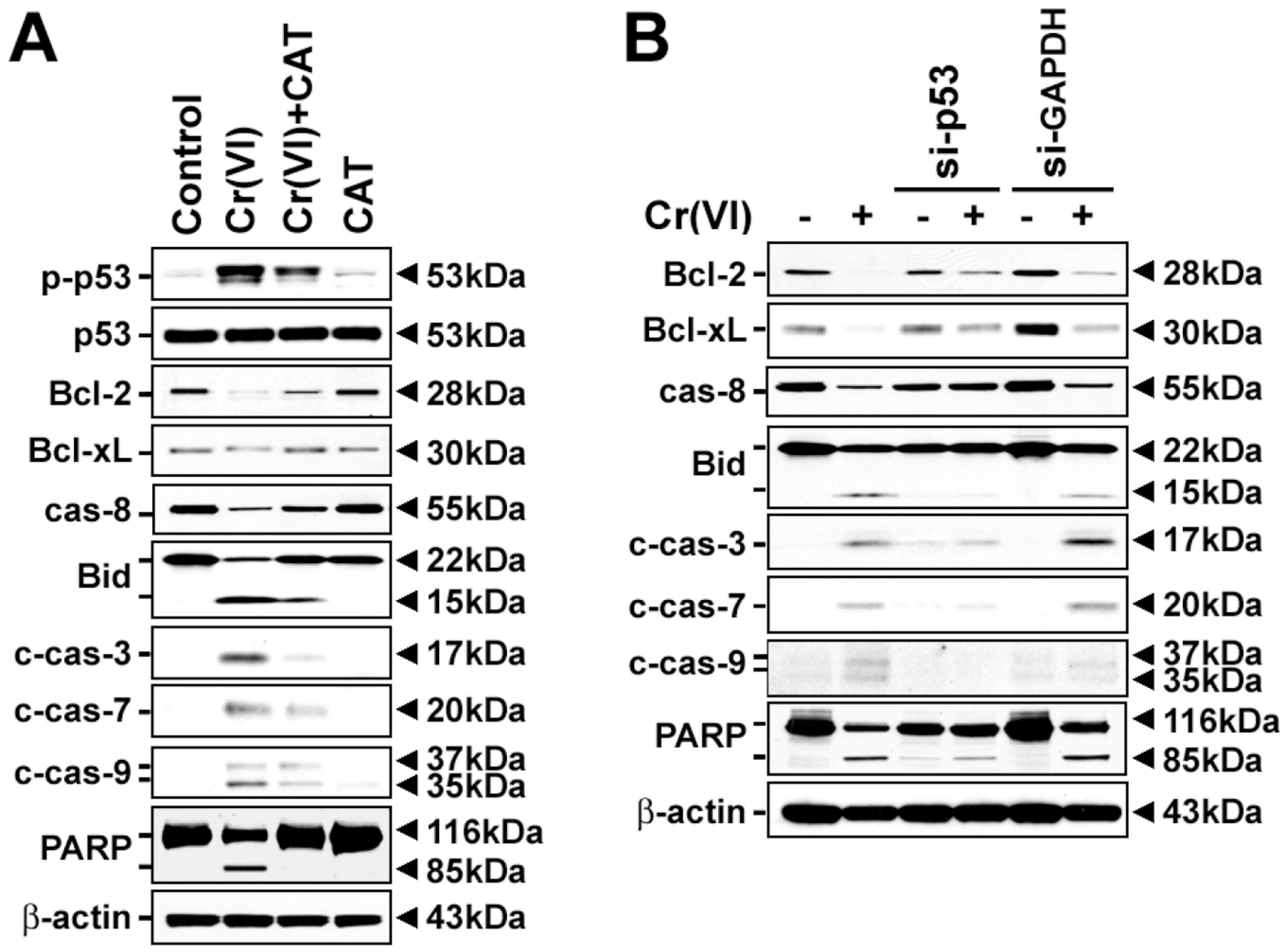

Fig. 8.

Cr(VI) induces ROS-dependent and p53-mediated apoptosis in JB6 cells. (A) The cells were exposed to 10 μM Cr(VI) in the presence of 500 U/ml CAT for 48 h and then cellular proteins were analyzed by western blotting. (B) JB6 cells transfected with si-p53 or si-GAPDH were incubated in the presence and absence of 10 μM Cr(VI) for 48 h and then processed for the analysis of apoptosis-related proteins by immunoblotting. A representative result from triplicate experiments was shown.

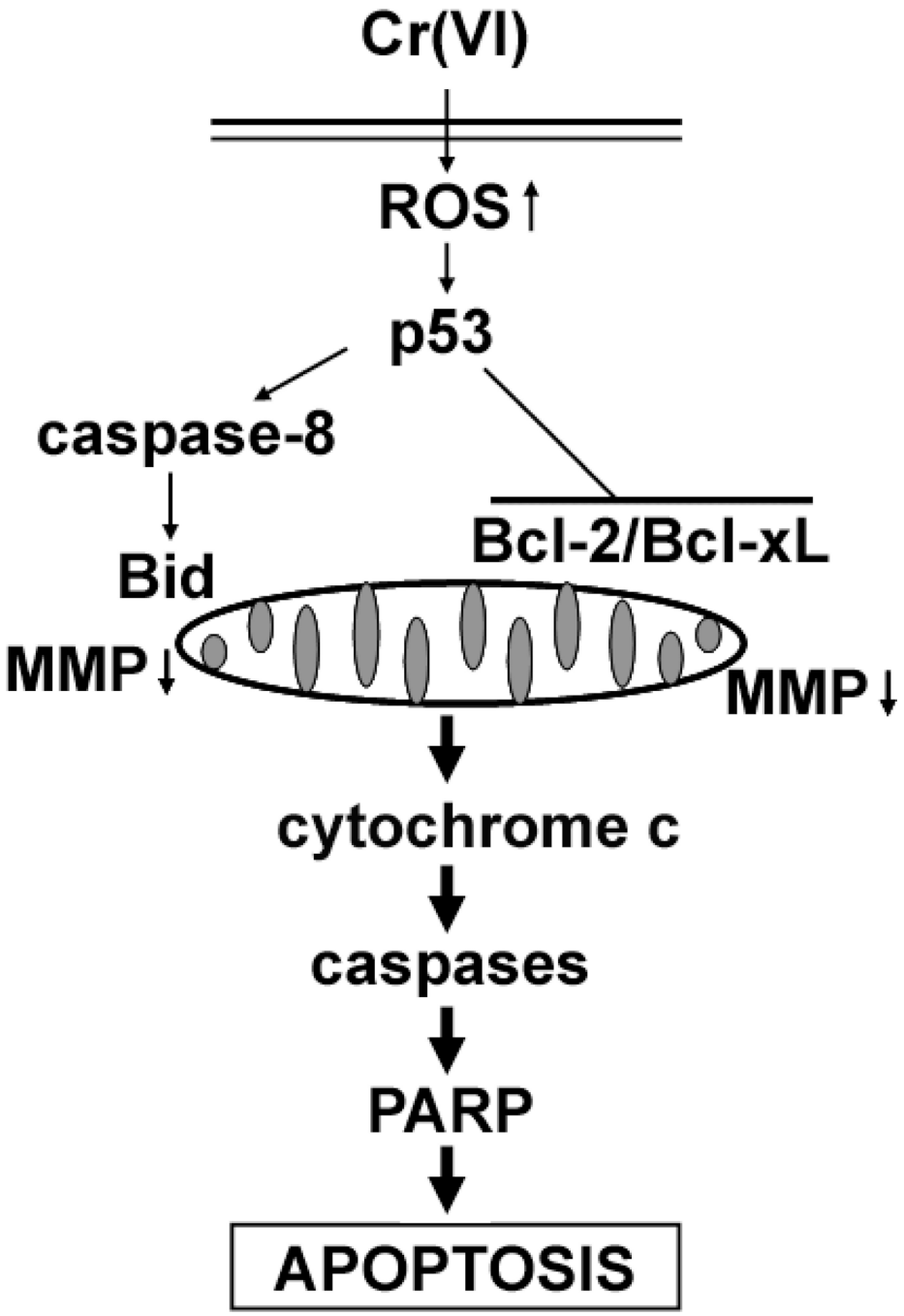

Fig. 9.
Cellular mechanisms involved in Cr(VI)-induced apoptosis in JB6 cells.